PHYSICAL REVIEW B **91**, 081106(R) (2015)

Tunable circular dichroism due to the chiral anomaly in Weyl semimetals

Pavan Hosur and Xiao-Liang Qi
Department of Physics, Stanford University, Stanford, California 94305, USA
(Received 28 January 2014; revised manuscript received 31 December 2014; published 17 February 2015)

Weyl semimetals are a three-dimensional gapless topological phase in which bands intersect at arbitrary points—the Weyl nodes—in the Brillouin zone. These points carry a topological quantum number known as the *chirality* and always appear in pairs of opposite chiralities. The notion of chirality leads to anomalous nonconservation of chiral charge, known as the *chiral anomaly*, according to which charge can be pumped between Weyl nodes of opposite chiralities by an electromagnetic field with nonzero $\boldsymbol{E}\cdot\boldsymbol{B}$. Here, we propose probing the chiral anomaly by measuring the optical activity of Weyl semimetals via circular dichroism. In particular, we observe that applying such an electromagnetic field on this state gives it a nonzero gyrotropic coefficient or a Hall-like conductivity, which may be detectable by routine circular dichroism experiments. This method also serves as a diagnostic tool to discriminate between Weyl and Dirac semimetals; the latter will give a null result. More generally, any experiment that probes a bulk correlation function that has the same symmetries as the gyrotropic coefficient can detect the chiral anomaly as well as differentiate between Dirac and Weyl semimetals.

DOI: 10.1103/PhysRevB.91.081106 PACS number(s): 78.20.Ek, 78.40.Kc

I. INTRODUCTION

Weyl semimetals (WSMs) are a novel gapless topological phase of matter that have accrued considerable attention as of late [1–4]. They are three-dimensional systems whose band structure contains isolated points in momentum space where a pair of nondegenerate bands intersect. These intersection points— or Weyl nodes—can be assigned a *handedness* or *chirality* $\chi = \pm 1$; very general arguments show that the total number of Weyl nodes in the Brillouin zone must be even with half of each chirality [5,6]. Moreover, they are topological in the sense that they can only be annihilated (gapped out) in pairs of opposite chirality, or via superconductivity. Thus, they are stable as long as translational symmetry and charge conservation hold. Near the Weyl nodes, the dispersion is linear and the Hamiltonian resembles the Hamiltonian for Weyl fermions well known in high-energy physics,

$$H_W = \chi \boldsymbol{k}\cdot\boldsymbol{\sigma}, \tag{1}$$

where $\boldsymbol{k}$ is the momentum relative to the Weyl node and σ_i are Pauli matrices in the local band basis—hence, the name WSMs.

WSMs are bestowed with a physical property known as the Adler-Bell-Jackiw anomaly or the chiral anomaly [7–14]. This is a well-known phenomenon in high-energy physics. It represents an anomalous nonconservation of chiral charge in the presence of appropriate external electromagnetic fields, even though the Hamiltonian enjoys the continuous symmetry—the chiral gauge symmetry—that is expected to lead to chiral charge conservation via Noether's theorem. The resolution to this paradox lies in the fact that the chiral gauge transformation modifies the integration measure in the path integral, and hence the path integral itself. Thus, the chiral anomaly is a purely quantum process that the classical Hamiltonian is oblivious to. Viewed differently, it is an artifact of the low-energy theory, and appropriate regularization at high energies that smoothly interpolates between Weyl Hamiltonians of opposite chiralities would destroy the chiral gauge symmetry [1].

WSMs present a condensed matter realization of the phenomenon. In this context, the anomaly implies that although the total charge in the WSM is conserved, the charge in the momentum states near the left-handed or the right-handed Weyl nodes is not individually conserved. In the simplest case of a WSM with just two Weyl nodes, the anomaly can be written as

$$\partial_\mu j^\mu_{\rm ch} = \frac{e^2}{4\pi^2\hbar^2}\boldsymbol{E}\cdot\boldsymbol{B}, \tag{2}$$

where $j^\mu_{\rm ch} = (j^\mu_+ - j^\mu_-)/2$ is the four-dimensional chiral current and the subscripts $\pm$ on the currents denote the chirality of the Weyl node contributing to them, and the right-hand side states that the pumping is driven by an electromagnetic field configuration with nonzero $\boldsymbol{E}\cdot\boldsymbol{B}$.[1] The electromagnetic fields are space and time dependent in general. In the absence of any spatial variations, (2) reduces to

$$\partial_t \rho_{\rm ch} = \frac{e^2}{4\pi^2\hbar^2}\boldsymbol{E}(t)\cdot\boldsymbol{B}(t). \tag{3}$$

For time-independent $\boldsymbol{E}$ and $\boldsymbol{B}$, $\rho_{\rm ch}$ grows linearly with time until a scattering process cuts off the growth by relaxing the charge imbalance between the Weyl nodes. Such processes are rare in clean systems since they involve a large momentum transfer. Thus, any measurement of the chiral anomaly can unambiguously distinguish between WSMs and the less exotic Dirac semimetals, in which Weyl nodes of opposite chiralities coincide in momentum and energy. Equation (2) is a two-dimensions-higher version of the chiral anomaly present at the edge of an integer quantum Hall state [15]. There, charge can be pumped from one edge to the other by a longitudinal electric field, $\partial_\mu j^\mu_{\rm ch} = \frac{e^2}{2\pi\hbar}E$. An important difference, however, is that the chiral currents $j^\mu_\pm$ in the integer quantum Hall state reside on spatially separated edges and can be observed individually

[1]Henceforth, we abbreviate "electromagnetic fields with nonzero $\boldsymbol{E}\cdot\boldsymbol{B}$" as "an $\boldsymbol{E}\cdot\boldsymbol{B}$ field" or parallel electric and magnetic fields.

 ©2015 American Physical Society

with local probes, whereas the chiral currents in WSMs are separated in momentum space and cannot be distinguished by spatially local probes. The question is, what kind of probe can qualitatively see the chiral anomaly?

A transport phenomenon intimately tied to the chiral anomaly that was noticed early on was a large longitudinal magnetoconductivity. This occurs because relaxation of chiral charge involves large momentum scattering and hence takes a long time in clean systems [7]. Recently, another transport experiment was proposed in which chiral charge pumping according to (3) resulted in a large enhancement of the length scale over which an applied local voltage decayed [16]. However, these effects are quantitative rather than qualitative and hence difficult to identify unambiguously in magnetotransport data [17], especially if the intervalley relaxation time is short. While the first effect is accompanied by weak localization or weak antilocalization physics [18] in $\mathcal{T}$-symmetric WSMs and would have to be isolated from it, the enhancement of the length scale in the second proposal may not be large enough to be measurable for moderate intervalley relaxation rates because the nonlocal voltage falls exponentially with the rate. There exist various other predictions for chiral transport phenomena, most famously a nonquantized anomalous Hall effect [3,11,13,19–22] and the *chiral magnetic effect* [9,19,23,24], in which a current flows along an applied magnetic field. An optical signature of the anomalous Hall effect, namely, anomalous birefringence, was briefly discussed in Ref. [25]. However, a more fundamental question remains unanswered, namely, what kinds of material properties are sensitive to the chirality of a given system? Experiments that measure these properties can, in principle, be designed to *qualitatively* rather than *quantitatively* probe the chiral anomaly in WSMs as well.

II. GYROTROPY

In this Rapid Communication, we propose that material parameters or transport coefficients that are of the form of time-reversal-invariant ($\mathcal{T}$-invariant) rank-3 pseudotensors are appropriate probes of the anomaly. Just like the chirality of a system, these quantities are odd under inversion ($\mathcal{I}$) and even under $\mathcal{T}$ and, hence directly couple to it. They can therefore be employed to distinguish between Weyl nodes of opposite chirality and consequently probe the chiral anomaly. Below, we elaborate on one such a material property—one which is responsible for optical activity. However, the fact that $\mathcal{T}$-invariant rank-3 pseudotensors exist only in chiral systems is more general and can be used to probe the chiral anomaly in other kinds of experiments as well. For instance, a chiral strain field, such as that present near a screw dislocation, will modify the resistivity by an amount that depends on the handedness of the dislocation as well as to the chirality of the underlying band structure. The relevant tensor for this phenomenon is the elastoresistive tensor, which describes the change in resistivity due to applied strain. On the other hand, these tensors, despite being nonvanishing in general in all chiral systems, are not tunable in ordinary chiral systems such as sugar molecules. It is only in WSMs that the chiral anomaly can be exploited to tune the magnitude and sign of chiral transport.

The $\mathcal{T}$-invariant rank-3 pseudotensor that is responsible for optical activity is the gyrotropic tensor γ_{ijk}, which is defined in terms of the dielectric tensor $\epsilon_{ij}(\boldsymbol{q},\omega)$ as [26]

$$\epsilon_{ij}(\boldsymbol{q},\omega) = \epsilon^0_{ij}(\omega) + i\gamma_{ijk}(\omega)q_k + O(q^2), \tag{4}$$

where $\boldsymbol{q}$ and ω are the wave vector and frequency of light. Clearly, γ_{ijk} represents the response to variations in the electric field. For systems with cubic or higher symmetry, such as a single isotropic Weyl node, this tensor is purely antisymmetric, $\gamma_{ijk} = \gamma\varepsilon_{ijk}$, and the gyrotropic coefficient reduces to a complex number γ. Similarly, the q-independent diagonal part of the dielectric tensor is proportional to the Kronecker delta function $\epsilon^0_{ij}(\omega) = \epsilon_0(\omega)\delta_{ij}$ for a single isotropic Weyl node. Isotropy of the Weyl node can be assumed without losing any essential physics, since any anisotropy can be removed by rescaling momenta around the node.

$\mathcal{T}$ symmetry leads to Onsager's reciprocity condition $\epsilon_{ij}(\boldsymbol{q},\omega) = \epsilon_{ji}(-\boldsymbol{q},\omega)$, which allows a nonzero γ, while mirror symmetries allow only even powers of momentum normal to the mirror plane in the dielectric tensor. Thus, γ vanishes in systems that have a mirror symmetry. Systems that break all mirror symmetries and hence break $\mathcal{I}$ symmetry have a nonvanishing γ in general and can be assigned a handedness proportional to γ. In particular, a single Weyl node is chiral and can have a nonzero $\gamma \propto \chi$. However, any symmetries relating Weyl nodes of opposite chiralities will make the total γ of the WSM vanish. Since spatially local probes only detect the total response of all the Weyl nodes, they will then see a null result for γ. To get a nonzero result, one must find a way to subtract, rather than add, contributions to γ from Weyl nodes of opposite chirality.

Such a subtraction can be done by observing that γ is related to the Hall conductivity through the relation $\epsilon_{ij} = \delta_{ij} + \frac{i\sigma_{ij}}{\varepsilon_0\omega}$, where ε_0 is the permittivity of free space, so it must have contributions that are odd in the charge of the quasiparticles. If one can somehow arrange for the doping to be different at the $\chi = +1$ and $\chi = -1$ Weyl nodes, their contributions to γ will no longer cancel. The anomaly induced by $\boldsymbol{E}\cdot\boldsymbol{B}$ [(2) and (3)] precisely ensures such a charge imbalance between the two chiralities. In other words, once a finite amount of charge has been pumped from $\chi = -1$ to $\chi = +1$, the $\chi = -1$ ($\chi = +1$) Weyl node is surrounded by a hole (electron) Fermi surface, assuming they were undoped initially, as shown in Fig. 1. If they were already doped, their local Fermi levels will become different. In the language of symmetries, chiral charge pumping ensures that all symmetries relating Weyl nodes of opposite chiralities are broken because they have different Fermi levels relative to the Weyl points.

That systems with nonzero γ exhibit circular dichroism—conversion of linearly polarized light into elliptically polarization as it propagates through the system—can be seen as follows. The eigenmodes of the dielectric tensor (4) correspond to circularly polarized light; the associated eigenvalues determine the refractive indices for the two polarizations, $n^2_{L,R}(\omega) = \epsilon_0(\omega) \pm \gamma q$. Later, we will find that γ for the system of interest is purely imaginary. Since $\mathrm{Im}(n_L) \neq \mathrm{Im}(n_R)$, the two circular polarizations making up the linear polarization are absorbed by different amounts as the light propagates through the system, resulting in circular dichroism. It is straightforward to show

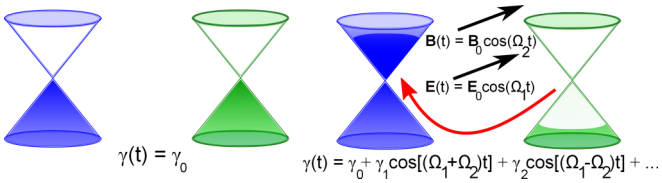

FIG. 1. (Color online) Illustration of gyrotropy induced by an $\boldsymbol{E}\cdot\boldsymbol{B}$ field in WSMs. Colored (white) regions denote filled (empty) states and the two colors indicate Weyl nodes of opposite chiralities, which are located at different points in momentum space. In the absence of $\boldsymbol{E}\cdot\boldsymbol{B}$, the Fermi levels at the two nodes are equal. An $\boldsymbol{E}\cdot\boldsymbol{B}$ field pumps charge across the nodes, shown by the curved red arrow, resulting in a charge imbalance between the nodes and a consequent net anomalous contribution to γ. Since WSMs break $\mathcal{I}$ or $\mathcal{T}$, they are in general optically active in the absence of external fields as well. The anomalous contribution, proportional to $\boldsymbol{E}\cdot\boldsymbol{B}$, can be isolated by applying electromagnetic fields at distinct finite frequencies.

that the ellipticity of the light that comes out is given by

$$|\tan\theta_{CD}| \equiv \left|\frac{E_R - E_L}{E_R + E_L}\right| \approx \frac{|\mathrm{Im}[\gamma]|\ell\omega^2}{2c^2} \tag{5}$$

for $|\gamma\omega/c| \ll \epsilon_0$, where $E_{L,R}$ are the transmitted amplitudes of the circularly polarized fields, ℓ is the thickness of the sample, and c is the speed of light. Thus, we propose detecting the chiral anomaly *optically*. Later in this Rapid Communication, we estimate the sizes of this effect for typical WSMs and find it may be within experimental limits.

A caveat, though, is that WSMs can at most preserve only one out of $\mathcal{I}$ and $\mathcal{T}$ symmetries. Consequently, a $\mathcal{T}$-symmetric WSM already has a nonzero γ in general, without external fields, while an $\mathcal{I}$-symmetric WSM has vanishing γ but can be optically active due to possible ferromagnetic moments that break $\mathcal{T}$. Later we will describe how the background contributions to optical activity can be separated from the anomaly-based ones by a clever separation of their frequencies.

III. SINGLE WEYL NODE RESULTS

In the following, we will first calculate the gyrotropic coefficient of a single Weyl node and then apply the results to WSMs with multiple Weyl nodes. We start with the Hamiltonian $H_{\boldsymbol{k}}^{\chi} = \chi\hbar v_F \boldsymbol{k}\cdot\boldsymbol{\sigma} - \mu_\chi$ for a single Weyl node W^χ of chirality χ and chemical potential μ_χ above the Weyl point. Such a description is valid if equilibration within a Weyl node occurs at time scales that are much shorter than the frequency at which the experiment is performed: $\omega \ll \tau_{\mathrm{intra}}^{-1}$. μ_χ consists of two parts in general, the background chemical potential due to doping already present in the system, and the change because of charge pumping. For a constant $\boldsymbol{E}\cdot\boldsymbol{B}$ field, which is what we assume for now, the latter grows linearly with time in the absence of large momentum scattering; in practice, such scattering *is* present and the system reaches a nonequilibrium steady state characterized by an intervalley relaxation time τ_{inter}. Equation (3) dictates that the density of electrons pumped into the neighborhood of W_χ in this time is $\Delta\rho_\chi = \chi\frac{e^2}{4\pi^2\hbar^2}\boldsymbol{E}\cdot\boldsymbol{B}\tau_{\mathrm{inter}}$. Later we argue that time-dependent fields greatly facilitate separating the anomalous contribution to γ from possible background terms, and modify the results accordingly.

In the low-frequency limit, $\omega\tau_{\mathrm{intra}} \ll 1$, γ_{ijk} was shown to be related to the first moment of the Berry curvature of the occupied states and is thus particularly easy to calculate [27]. We recap the derivation below following a similar spirit as Ref. [27], keeping the application to a single Weyl node in mind.

The semiclassical equations of motion for a wave packet in a band with dispersion $\varepsilon(\boldsymbol{k})$ and Berry curvature $\boldsymbol{F}(\boldsymbol{k}) = i\nabla_{\boldsymbol{k}}\times\langle\psi_{\boldsymbol{k}}|\nabla_{\boldsymbol{k}}\psi_{\boldsymbol{k}}\rangle$, where $|\psi_{\boldsymbol{k}}\rangle$ is the Bloch wave function, in the presence of a space-time varying electric field $\boldsymbol{E}(\boldsymbol{r},t) = \boldsymbol{E}e^{i(\boldsymbol{q}\cdot\boldsymbol{r}-\omega t)}$, read

$$\dot{\boldsymbol{r}} = \boldsymbol{v}(\boldsymbol{k}) - \boldsymbol{F}(\boldsymbol{k})\times\frac{e}{\hbar}\boldsymbol{E}(\boldsymbol{r},t), \quad \dot{\boldsymbol{k}} = \frac{e}{\hbar}\boldsymbol{E}(\boldsymbol{r},t), \tag{6}$$

where $\boldsymbol{v}(\boldsymbol{k}) = \frac{1}{\hbar}\nabla_{\boldsymbol{k}}\varepsilon(\boldsymbol{k})$. The second term above describes the anomalous Hall current [28]; integrating over $\boldsymbol{k}$ gives a Hall current at $\boldsymbol{r}$ due to the local electric field at $\boldsymbol{r}$. However, gyrotropy stems from a Hall-like response driven by spatial variations in the electric field. Such a response is nonlocal, and requires solving (6) for finite times. Doing so iteratively to first order in $\boldsymbol{E}$ yields

$$\begin{aligned}\boldsymbol{r}(t) &= \boldsymbol{r}_0 + \boldsymbol{v}(\boldsymbol{k}_0)t \\ &\quad + \int_0^t dt'\int_0^{t'} dt''\frac{e}{\hbar}\boldsymbol{E}(\boldsymbol{r}_0+\boldsymbol{v}(\boldsymbol{k}_0)t'',t'')\cdot\nabla_{\boldsymbol{k}_0}\boldsymbol{v}(\boldsymbol{k}_0) \\ &\quad - \frac{e}{\hbar}\boldsymbol{F}_{\boldsymbol{k}_0}\int_0^t dt'\boldsymbol{E}(\boldsymbol{r}_0+\boldsymbol{v}(\boldsymbol{k}_0)t',t'), \\ \boldsymbol{k}(t) &= \boldsymbol{k}_0 + \int_0^t dt'\frac{e}{\hbar}\boldsymbol{E}(\boldsymbol{r}_0+\boldsymbol{v}(\boldsymbol{k}_0)t',t'),\end{aligned} \tag{7}$$

where $\boldsymbol{r}_0$ and $\boldsymbol{k}_0$ are the initial position and wave vector of the wave packet. The Hall response is given by the third line of the expression for $\boldsymbol{r}(t)$. Explicitly, it is

$$\boldsymbol{j}_{\mathrm{Hall}}(\boldsymbol{k}_0,t) = e\dot{\boldsymbol{r}}_{\mathrm{Hall}}(\boldsymbol{k}_0,t) = \boldsymbol{E}(\boldsymbol{r},t)e^{i\boldsymbol{q}\cdot\boldsymbol{v}_{\boldsymbol{k}_0}t}\frac{e^2}{\hbar}\boldsymbol{F}_{\boldsymbol{k}_0}. \tag{8}$$

Integrating over $\boldsymbol{k}_0$ for all occupied states gives the total Hall current density

$$\boldsymbol{J}_{\mathrm{Hall}}(\boldsymbol{r},t) \approx \frac{e^2}{\hbar}\boldsymbol{E}(\boldsymbol{r},t)\int_{\boldsymbol{k}\in\mathrm{occ}}\boldsymbol{F}_{\boldsymbol{k}}(1+i\boldsymbol{q}\cdot\boldsymbol{v}_{\boldsymbol{k}}t) \tag{9}$$

for $|\boldsymbol{q}\cdot\boldsymbol{v}_{\boldsymbol{k}}t| \ll 1$. For a single Weyl node doped away from the Weyl point, the first term vanishes because of an effective time-reversal symmetry in H_χ, $\boldsymbol{k}\to-\boldsymbol{k}$, $\boldsymbol{\sigma}\to-\boldsymbol{\sigma}$, which results in $\boldsymbol{F}_{\boldsymbol{k}} = -\boldsymbol{F}_{-\boldsymbol{k}}$. The nonvanishing part of the γ, proportional to the $\boldsymbol{q}$-linear part of the Hall conductivity, is

$$\gamma_{\mathrm{single}}(\omega) = \frac{e^2}{\hbar}\frac{i\tau_{\mathrm{intra}}}{\varepsilon_0\omega}\int_{\boldsymbol{k}\in\mathrm{occ}}(\boldsymbol{F}_{\boldsymbol{k}}\cdot\hat{\boldsymbol{q}})(\boldsymbol{v}_{\boldsymbol{k}}\cdot\hat{\boldsymbol{q}}). \tag{10}$$

In writing (10), we have replaced t by τ_{intra} to suggest that the linear growth with time is cut off by a relaxation process at $t \simeq \tau_{\mathrm{intra}}$. The physical meaning of the above result is as follows. Imagine a pair of electrons, with momentum $\boldsymbol{k}$ and $-\boldsymbol{k}$, starting at the same point in space and traveling in opposite directions, along $\boldsymbol{q}$ and along $-\boldsymbol{q}$. They can travel for a time τ_{intra} without getting scattered; in the process, they are acted upon by slightly different electric fields since the electric field

varies in space. Since the Berry curvatures they experience are equal and opposite, their total contribution to the Hall current is nonvanishing and proportional to the wave vector corresponding to the electric field variations. For a single Weyl node given by the Hamiltonian $H_{\boldsymbol{k}}^{\chi} = \chi \hbar v_F \boldsymbol{k} \cdot \boldsymbol{\sigma} - \mu_\chi$, it is straightforward to show that $\boldsymbol{F_k} = \chi \frac{\hat{\boldsymbol{k}}}{2k^2}$ and $\boldsymbol{v_k} = v_F \hat{\boldsymbol{k}}$. Substituting in (10) gives

$$\gamma_{\text{single}}(\omega) = i \frac{\chi \mu_\chi e^2 \tau_{\text{intra}}}{6\pi^2 \varepsilon_0 \hbar^2 \omega}. \tag{11}$$

Note that γ_{single} is purely imaginary, so it leads to circular dichroism.

IV. APPLYING TO REAL WSM

Having derived γ for a single Weyl node, we now make the leap to a real WSM, which contains an even number of Weyl nodes with half of each chirality. Thus, we sum the contributions of all the Weyl nodes and estimate the size of the consequent gyrotropic circular dichroism in a real WSM. For simplicity, we assume an $\mathcal{I}$-symmetric system with two Weyl nodes, one of each chirality. The results can be trivially scaled to N pairs of nodes by simply multiplying by N. If the Fermi level is tuned to the Weyl point in the absence of external electromagnetic fields—the iridate (candidate) WSMs $Y_2Ir_2O_7$ and $Eu_2Ir_2O_7$ are expected to be in this limit because of their stoichiometry—then there is no background chemical potential and μ_χ only depends on the charge pumped:

$$\mu_\chi = \chi \left(\frac{3e^2 \hbar v_F^3}{2} \boldsymbol{E} \cdot \boldsymbol{B} \tau_{\text{inter}} \right)^{1/3}. \tag{12}$$

Summing (11) for two nodes gives

$$\gamma(\omega) = i \frac{e^2 \tau_{\text{intra}}}{3\pi^2 \varepsilon_0 \hbar^2 \omega} \left(\frac{3e^2 \hbar v_F^3}{2} \boldsymbol{E} \cdot \boldsymbol{B} \tau_{\text{inter}} \right)^{1/3} \tag{13}$$

and

$$|\tan\theta_{CD}| = \frac{\alpha}{3\pi} (\omega \tau_{\text{inter}}) \frac{|\mu_+ - \mu_-| \ell}{\hbar c}, \tag{14}$$

where $\alpha = e^2/4\pi\varepsilon_0 \hbar c \approx 1/137$ is the fine structure constant. Putting in realistic values of parameters, $v_F \approx 10^6$ ms^{-1} from the band structure of candidate WSMs $Y_2Ir_2O_7$, $Eu_2Ir_2O_7$ [29], and Cd_3As_2 [30], $|\boldsymbol{E}| = 10$ V/mm, $|\boldsymbol{B}| = 1$ T, $\tau_{\text{intra}} = 1$ fs, $\tau_{\text{inter}} = 100$ ps, $\hbar\omega = 100$ meV, $\ell \sim 1$ μm gives $|\mu_\chi| \sim 10$ meV and $|\tan\theta_{CD}| \sim 10$ μrad. We have chosen numbers so that ω exceeds the plasma frequency $\omega_p \simeq \sqrt{(2\alpha/3\pi)(c/v_F)}|\mu_\chi|$ [31,32]; this ensures that the incident light is not screened. While the above estimate is crude, it suggests that the effect may be measurable by current experiments. Moreover, the effect will be enhanced in a sufficiently clean system since both the lifetimes τ_{inter} and τ_{intra} will be longer.

On the other hand, if the WSM is doped to a Fermi level of ϵ_F away from the Weyl nodes, the effect is suppressed by $O[(\frac{\mu_+ - \mu_-}{\epsilon_F})^2]$ for the same amount of charge pumped because of the density of states for a three-dimensional linear dispersion is proportional to ϵ^2. Moreover, choosing a frequency that lies between τ_{intra}^{-1} and ω_p will be difficult and perhaps impossible. Thus, we only focus of the case where the WSM is undoped to begin with.

V. SUBTRACTING THE BACKGROUND

Circular dichroism measurements are commonly used to study systems that break $\mathcal{T}$ or $\mathcal{I}$ symmetry. WSMs break at least one of $\mathcal{T}$ and $\mathcal{I}$ symmetries, and thus exhibit intrinsic, i.e., $\boldsymbol{E} \cdot \boldsymbol{B}$-independent, optical activity in general. The final piece of the puzzle of probing the anomaly via gyrotropy is being able to subtract this background.

One way to do so is to simply do an experiment without $\boldsymbol{E}$ and $\boldsymbol{B}$ fields and subtract the results from the results in the presence of an $\boldsymbol{E} \cdot \boldsymbol{B}$ field. While this procedure can work in principle, it involves subtracting a potentially large background and is thus error prone. Moreover, the $\boldsymbol{E}$ and $\boldsymbol{B}$ fields can change the optical activity independently of the chiral anomaly as well, for instance, by inducing polarization or magnetization.

A cleaner procedure would be to make the fields time dependent. Thus, if one applies $\boldsymbol{E}(t) = \boldsymbol{E} \cos \Omega_1 t$ and $\boldsymbol{B}(t) = \boldsymbol{B} \cos \Omega_2 t$, such that $\Omega_{1,2} \ll \tau_{\text{inter}}^{-1}$, and measures the optical activity at a higher frequency $\omega \gg \tau_{\text{inter}}^{-1}$, then $\boldsymbol{E}(t)$ and $\boldsymbol{B}(t)$ can be treated quasistatically and the preceding analysis can be applied with minor modifications. In particular, the gyrotropic coefficient will pick up a slow time dependence,

$$\gamma(\omega; t) = \frac{4i\alpha c \tau_{\text{intra}}}{3\pi\hbar\omega} \left(\frac{3e^2 \hbar v_F^3 \tau_{\text{inter}}}{2} \boldsymbol{E} \cdot \boldsymbol{B} \cos \Omega_1 t \cos \Omega_2 t \right)^{1/3}, \tag{15}$$

for $\tau_{\text{inter}} \ll t \ll \Omega_{1,2}^{-1}$, and will thus have components at frequencies $\Omega_1 \pm \Omega_2$ which should be easily separable from other frequency components. In addition to the time dependence of γ, its dependence on the relative angle between $\boldsymbol{E}$ and $\boldsymbol{B}$ should be easy to observe as well on top of the constant background.

VI. CONCLUSIONS

In summary, we have described a method to probe the chiral anomaly in WSMs optically. Our method is based on the fact that an $\boldsymbol{E} \cdot \boldsymbol{B}$ electromagnetic field in a WSM produces a charge imbalance between Weyl nodes of opposite chiralities. Such an imbalance gives rise to a nonzero gyrotropic coefficient γ, a Hall-like contribution to the dielectric tensor which determines the optical activity of the system. A routine circular dichroism experiment can then potentially detect the effect. We show how applying time-dependent $\boldsymbol{E}$ and $\boldsymbol{B}$ fields facilitates the isolation of the anomalous contributions to the optical activity from possible nonanomalous ones. Additionally, anomalous optical activity distinguishes between Dirac and Weyl semimetals. In particular, Dirac semimetals do not exhibit a chiral anomaly and thus cannot develop an $\boldsymbol{E} \cdot \boldsymbol{B}$ induced valley imbalance. However, unlike in WSMs, even preexisting valley imbalances in Dirac semimetals do not contribute to γ since Dirac nodes are achiral while γ is directly sensitive to the chirality of the system. We estimate the typical size of the anomalous circular dichroism in WSMs and find it to be accessible by current experiments. Finally, we point out that other experiments that can measure material parameters

that have the same symmetries as the gyrotropic coefficient can also be used to probe the chiral anomaly in WSMs as well as to distinguish them from Dirac semimetals.

ACKNOWLEDGMENT

We would like to thank the David and Lucile Packard Foundation for financial support.

[1] P. Hosur and X. Qi, C. R. Phys. **14**, 857 (2013).
[2] W. Witczak-Krempa and Y.-B. Kim, Phys. Rev. B **85**, 045124 (2012).
[3] O. Vafek and A. Vishwanath, Annu. Rev. Condens. Matter Phys. **5**, 83 (2014).
[4] A. M. Turner and A. Vishwanath, arXiv:1301.0330.
[5] H. B. Nielsen and M. Ninomiya, Nucl. Phys. B **185**, 20 (1981).
[6] H. B. Nielsen and M. Ninomiya, Nucl. Phys. B **193**, 173 (1981).
[7] H. B. Nielsen and M. Ninomiya, Phys. Lett. B **130**, 389 (1983).
[8] V. Aji, Phys. Rev. B **85**, 241101 (2012).
[9] G. Basar, D. E. Kharzeev, and H.-U. Yee, Phys. Rev. B **89**, 035142 (2014).
[10] D. T. Son and B. Z. Spivak, Phys. Rev. B **88**, 104412 (2013).
[11] A. A. Zyuzin and A. A. Burkov, Phys. Rev. B **86**, 115133 (2012).
[12] K. Landsteiner, Phys. Rev. B **89**, 075124 (2014).
[13] P. Goswami and S. Tewari, Phys. Rev. B **88**, 245107 (2013).
[14] P. Hosur, S. A. Parameswaran, and A. Vishwanath, Phys. Rev. Lett. **108**, 046602 (2012).
[15] N. Maeda, Phys. Lett. B **376**, 142 (1996).
[16] S. A. Parameswaran, T. Grover, D. A. Abanin, D. A. Pesin, and A. Vishwanath, Phys. Rev. X **4**, 031035 (2014).
[17] H.-J. Kim, K.-S. Kim, J. F. Wang, M. Sasaki, N. Satoh, A. Ohnishi, M. Kitaura, M. Yang, and L. Li, Phys. Rev. Lett. **111**, 246603 (2013).
[18] I. Garate and L. Glazman, Phys. Rev. B **86**, 035422 (2012).
[19] Y. Chen, S. Wu, and A. A. Burkov, Phys. Rev. B **88**, 125105 (2013).
[20] G. Xu, H. M. Weng, Z. Wang, X. Dai, and Z. Fang, Phys. Rev. Lett. **107**, 186806 (2011).
[21] K.-Y. Yang, Y.-M. Lu, and Y. Ran, Phys. Rev. B **84**, 075129 (2011).
[22] A. A. Burkov and L. Balents, Phys. Rev. Lett. **107**, 127205 (2011).
[23] J.-H. Zhou, J. Hua, N. Qian, and S. Jun-Ren, Chin. Phys. Lett. **30**, 027101 (2013).
[24] M. M. Vazifeh and M. Franz, Phys. Rev. Lett. **111**, 027201 (2013).
[25] A. G. Grushin, Phys. Rev. D **86**, 045001 (2012).
[26] L. Landau, E. Lifshitz, E. Lifshitz, and L. Pitaevski, *Electrodynamics of Continuous Media* (Pergamon, New York, 1984).
[27] J. E. Moore and J. Orenstein, Phys. Rev. Lett. **105**, 026805 (2010).
[28] F. D. M. Haldane, Phys. Rev. Lett. **93**, 206602 (2004).
[29] X. Wan, A. M. Turner, A. Vishwanath, and S. Y. Savrasov, Phys. Rev. B **83**, 205101 (2011).
[30] Z. Wang, H. Weng, Q. Wu, X. Dai, and Z. Fang, Phys. Rev. B **88**, 125427 (2013).
[31] S. Das Sarma and E. H. Hwang, Phys. Rev. Lett. **102**, 206412 (2009).
[32] M. Lv and S.-C. Zhang, Int. J. Mod. Phys. B **27**, 1350177 (2013).